



THE UNIVERSITY *of* EDINBURGH

Edinburgh Research Explorer

## Channel Estimation for Spatial Modulation

**Citation for published version:**

Wu, X, Claussen, H, Di Renzo, M & Haas, H 2014, 'Channel Estimation for Spatial Modulation' IEEE Transactions on Communications, vol. 62, no. 12, pp. 4362-4372. DOI: 10.1109/TCOMM.2014.2366750

**Digital Object Identifier (DOI):**

[10.1109/TCOMM.2014.2366750](https://doi.org/10.1109/TCOMM.2014.2366750)

**Link:**

[Link to publication record in Edinburgh Research Explorer](#)

**Document Version:**

Peer reviewed version

**Published In:**

IEEE Transactions on Communications

**General rights**

Copyright for the publications made accessible via the Edinburgh Research Explorer is retained by the author(s) and / or other copyright owners and it is a condition of accessing these publications that users recognise and abide by the legal requirements associated with these rights.

**Take down policy**

The University of Edinburgh has made every reasonable effort to ensure that Edinburgh Research Explorer content complies with UK legislation. If you believe that the public display of this file breaches copyright please contact [openaccess@ed.ac.uk](mailto:openaccess@ed.ac.uk) providing details, and we will remove access to the work immediately and investigate your claim.



# Channel Estimation for Spatial Modulation

Xiping Wu\*, Holger Claussen<sup>†</sup>, Marco Di Renzo<sup>‡</sup>, and Harald Haas\*

\**Institute for Digital Communications, Joint Research Institute for Signal and Image Processing*

*School of Engineering, The University of Edinburgh, EH9 3JL, Edinburgh, UK*

<sup>†</sup>*Autonomous Networks and Systems Research Department, Bell Labs, Alcatel-Lucent*

*Blanchardstown Business and Technology Park, Dublin 15, Ireland*

<sup>‡</sup>*French National Centre for Scientific Research, Laboratory for Signals and Systems, École Supérieure d'Électricité*

*(SUPELEC), 3 rue Joliot-Curie, 91192 Gif-sur-Yvette (Paris), France*

{xiping.wu, h.haas}@ed.ac.uk, holger.claussen@alcatel-lucent.com, marco.direnzo@lss.supelec.fr

**Abstract**—In this paper, a novel channel estimation (CE) method is proposed for spatial modulation (SM), a unique single-stream, Multiple-Input Multiple-Output (MIMO) transmission technique. In SM, there is only one transmit antenna being active at any time instance. While this property completely avoids inter-channel interference, it results in a challenge to estimate the channel information. In conventional channel estimation (CCE) methods for SM, all transmit antennas have to be sequentially activated for sending pilots. Therefore, the time consumed in CE is proportional to the number of transmit antennas, which significantly compromises the throughput. By exploiting channel correlation, the proposed method, named transmission cross channel estimation (TCCE), has the following characteristics: i) the entire channel is estimated by sending pilots through one transmit antenna; ii) it requires no overhead or feedback; iii) it achieves a low computational complexity at the receiver. In addition, we propose an analytical framework to compute the distribution of the CE errors over time-varying fading channels. The corresponding Average Bit Error Probability (ABEP) bound of SM is also derived for the proposed method. Results show that the proposed ABEP bound matches with the simulations very well. When compared with CCE, the new method obtains a Signal-to-Noise Ratio (SNR) gain of up to 7.5 dB for medium and high correlations between the transmit antennas. Moreover, an adaptive CE technique can be readily implemented for SM via switching between CCE and TCCE.

**Index Terms**—Spatial modulation, MIMO, channel estimation, channel correlation, time-varying channel

## I. INTRODUCTION

Spatial modulation (SM) is a unique single-stream transmission technique for Multiple-Input Multiple-Output (MIMO) wireless communication systems [2]–[4]. In SM, the locations of the transmit antennas are used to carry information as well as the traditional signal modulation. Therefore, compared with single antenna systems, SM achieves an increase of the spectral efficiency by the factor of the base-two logarithm of the transmit antenna number. More importantly, only one transmit antenna is active at any given time in SM, which completely avoids inter-channel interference encountered in traditional MIMO systems. Furthermore, SM only requires a single radio-frequency (RF) chain, regardless of the number of transmit antennas used. This key property makes SM a truly energy-efficient technique for large scale MIMO systems. Recent research on SM has focused on studying its bit error ratio (BER) performance over fading channels with the

assumption of perfect channel state information (CSI) [5]–[7]. Results show that SM offers a better performance than many state-of-the-art (SOTA) MIMO techniques while allowing a low-complexity implementation.

However, perfect channel knowledge is always impractical and channel estimation (CE) is of vital importance that can not be neglected. In order to obtain the CSI at the receiver, pilot-based CE [8] is commonly used where pilots, i.e. deterministic symbols, are conveyed followed by the symbols carrying information. The pilot ratio is defined as the ratio of the number of pilots to the number of total symbols. Unlike multi-stream MIMO schemes such as vertical Bell Labs layered space-time (VBLAST) [9] and space-time block coding (STBC) [10], SM can send the pilots through only one antenna at a time. This challenges the channel estimation process for SM which has to sequentially activate the transmit antennas for sending pilots. We refer to this method as the conventional channel estimation (CCE), of which the pilot ratio is proportional to the number of transmit antennas. Unfortunately, this fact has so far been neglected in the SOTA literature. In [11] and [12], the BER performance of SM with imperfect CSI is respectively studied for uncorrelated and correlated fading channels. A similar work on space shift keying (SSK) is proposed in [13], where different lengths of the pilot sequence are considered. Although the above papers fill some gaps in the knowledge, they have the following limitations: i) the CE errors are arbitrary without considering practical CE methods; ii) the relation between the pilot ratio and the number of transmit antennas is not addressed. Until now, only a few studies have been conducted in studying CE techniques for SM. In [14], recursive least square (RLS) is investigated for MIMO systems based on a single RF chain. Another CE method for SM is proposed in [15], in which joint channel estimation with data detection is applied. However, these methods are developed based on existing CE techniques, and the issue of costly CE time is unsolved. It appears that no CE method specially tailored for SM has so far been proposed.

Because of the limited separation between antennas, MIMO channels are normally correlated to some degree in practical systems. This causes a degradation in the BER performance for all MIMO schemes including SM. Therefore, CE in this situation is required to be more accurate than that of uncorrelated channels. To date, most research in this area has focused on the optimal design of training signals [16]–[18]. Few estimators

<sup>1</sup>This paper was presented in part at the IEEE PIMRC 2013 [1].

are specially designed for correlated MIMO channels, and those few are based on specific channel correlation models [19], [20]. Due to the complexity and uncertainty of channel models in practical systems, the viability of those methods is limited. In addition to spatial correlation, time-varying is another challenge in channel estimation. With the aim of coping with time-varying MIMO channels, sequential channel estimation is proposed in [21], which is based on random-set theory. However, to the best of the authors' knowledge, no channel estimation method has so far been proposed to exploit the temporal and spatial channel correlation together.

In this paper, we aim to improve the CE performance for SM by exploiting the channel correlation information in both space and time. A novel CE approach, named transmission cross channel estimation (TCCE), is proposed. Unlike CCE, the new method estimates the whole MIMO channel by sending pilots through only one transmit antenna. As a result, the CE time is significantly reduced. More importantly, the proposed method requires no overhead or feedback, while achieving a low computational complexity at the receiver. Further, we propose an analytical framework to compute the distribution of the CE errors for time-varying channels. The corresponding Average Bit Error Probability (ABEP) bound is also derived for SM. Simulation results show that when the channel correlation between transmit antennas is larger than 0.35, TCCE offers a better performance than CCE with an Signal-to-Noise Ratio (SNR) gain of up to 7.5 dB. Moreover, an adaptive CE approach is available for SM by switching between CCE and TCCE.

The remainder of this paper is organized as follows. Section II describes the system model, including the SM transmitter, the channel model, and the receiver. The novel CE approach for SM is proposed in Section III. Section IV proposes a framework to compute the distribution of the CE errors for time-varying channels. In Section V, we derive the ABEP bound for SM associated with the proposed CE method. Simulation results are presented in Section VI, and the paper is concluded in Section VII.

## II. SYSTEM MODEL

### A. Spatial Modulation

An  $N_t \times N_r$  SM-MIMO system is considered, where  $N_t$  and  $N_r$  are the number of transmit antennas and the number of receive antennas, respectively. The information to be conveyed is separately carried by the spatial constellation diagram and signal constellation diagram. The size of the spatial constellation diagram is exactly the number of transmit antennas, while the size of the signal constellation diagram is denoted by  $M$ . The bit stream is divided into blocks of  $\eta_s$  bits, where  $\eta_s = \log_2(N_t M)$  is the number of bits per symbol. Each block is then split into two units of  $\log_2(N_t)$  and  $\log_2(M)$  bits and: i) the first segment activates one of the transmit antennas, and we denote the currently active antenna by  $t_{\text{act}}$ ; ii) the remaining bits are used to determine a symbol in the signal constellation diagram, and the active antenna conveys this symbol that is denoted by  $\chi_l$ ,  $l = 1, 2, \dots, M$ . The transmitted signal is expressed by a vector  $\mathbf{x}_{t_{\text{act}},l} = [x_1, x_2, \dots, x_{N_t}]^T$ , of which the  $t_{\text{act}}$ -th element carries  $\chi_l$  and all other elements are zero.

### B. Channel Model

In this paper, we consider a time-varying and spatially-correlated MIMO channel. The fading coefficient of the link between the  $t$ -th transmit antenna and the  $r$ -th receive antenna is denoted by  $h_{r,t(n)}$ , where  $n$  is the discrete time index. The corresponding  $N_r \times N_t$  channel matrix, denoted by  $\mathbf{H}_{(n)}$ , is generated in two stages: i) create a channel matrix of spatial correlation for the initial time, i.e.  $\mathbf{H}_{(0)}$ ; ii) yield a consecutive channel based on the temporal correlation, while maintaining the spatial correlation. It is worth noting that the proposed CE method is not restricted to a specific channel model. The channel model in this paper is for the purpose of theoretical analysis and performance validation for the proposed method. The study of different channel models is outside the scope of this paper.

1) *Spatial correlation*: The Kronecker model is widely used to generate spatially-correlated channels [22]. According to this model, the channel matrix is initialized as:

$$\mathbf{H}_{(0)} = \mathbf{R}_r^{1/2} \mathbf{G} \left( \mathbf{R}_t^{1/2} \right)^H, \quad (1)$$

where  $\mathbf{G}$  has the same dimension as  $\mathbf{H}_{(0)}$ , and its entries are independent and identically distributed (i.i.d.) complex Gaussian distribution  $\mathcal{CN}(0, 1)$ ;  $\mathbf{R}_t$  and  $\mathbf{R}_r$  denote the transmit correlation matrix and the receive correlation matrix, respectively. In this paper, the CE methods involved are individually implemented at each receive antenna. Therefore, the receive antennas are assumed to be independent without loss of generality, i.e.  $\mathbf{R}_r$  is an  $N_r \times N_r$  identity matrix. The correlation coefficient between the  $t_1$ -th and  $t_2$ -th transmit antennas is denoted by  $\rho_{t_1, t_2}$ , and the transmit correlation matrix is written as:

$$\mathbf{R}_t = \begin{bmatrix} 1 & \rho_{1,2} & \cdots & \rho_{1,N_t} \\ \rho_{2,1} & 1 & \cdots & \rho_{2,N_t} \\ \vdots & \vdots & \ddots & \vdots \\ \rho_{N_t,1} & \rho_{N_t,2} & \cdots & 1 \end{bmatrix} \quad (2)$$

The exponential correlation model in [23] is considered, which is based on the fact that the spatial correlation decreases as the distance between antennas increases. We use  $d_{t_1, t_2}$  to represent the Euclidean distance between  $t_1$  and  $t_2$ , and  $d$  is the reference distance. Then the correlation coefficient between two transmit antennas can be expressed as:

$$\rho_{t_1, t_2} = \rho \frac{d_{t_1, t_2}}{d}, \quad (3)$$

where  $\rho$  is the correlation degree when two antennas are separated at the reference distance.

2) *Temporal correlation*: The Gauss-innovations channel model in [24] is used to establish time-varying channels. The channel matrix at the  $n$ -th time index is formulated as follows:

$$\mathbf{H}_{(n)} = \sqrt{\alpha} \mathbf{H}_{(n-1)} + \sqrt{1-\alpha} \mathbf{H}'_{(n)}, \quad (4)$$

where  $\alpha$  is a parameter related to the user speed, and it is given by [24, Eq. (10)]:

$$\alpha = J_0 \left( \frac{2\pi v f_c T_s}{c} \right)^2, \quad (5)$$

where  $J_0(\cdot)$  is the zeroth-order Bessel function of the first kind;  $T_s$  is the sampling period;  $f_c$  is the center carrier frequency;  $v$  and  $c$  denote the speed of mobile user and the speed of light, respectively. The term  $\mathbf{H}'_{(n)}$  is also generated from (1), but it is independent of  $\mathbf{H}_{(n-1)}$ . In addition,  $\mathbf{H}'_{(n)}$  is independent from time to time. Substituting (1) into (4), we have:

$$\mathbf{H}_{(1)} = \mathbf{R}_r^{1/2} \left( \sqrt{\alpha} \mathbf{G}_{(0)} + \sqrt{1-\alpha} \mathbf{G}'_{(1)} \right) \left( \mathbf{R}_t^{1/2} \right)^H \quad (6)$$

It is straightforward to infer that  $\mathbf{H}_{(n)}$  is a correlated Rayleigh fading channel of the same correlation matrices as  $\mathbf{H}_{(0)}$ . Note that the above model also suits spatially-uncorrelated and/or time-invariant channels, by setting the correlation coefficients and/or the speed of mobile user to be zero.

### C. Maximum Likelihood Optimum Detector

We denote the noise at the input of the  $r$ -th receive antenna by  $w_r$ , which is assumed to be a complex Additive White Gaussian Noise (AWGN) process with distribution  $\mathcal{CN}(0, N_0)$ . Across the receive antennas, the noise components are statistically independent and denoted by  $\mathbf{w} = [w_1, w_2, \dots, w_{N_r}]^T$ . The received signal is given by:

$$\mathbf{y} = \mathbf{h}_{t_{\text{act}}} \chi_l + \mathbf{w}, \quad (7)$$

where  $\mathbf{y} = [y_1, y_2, \dots, y_{N_r}]^T$  and  $\mathbf{h}_{t_{\text{act}}}$  is the  $t_{\text{act}}$ -th column of  $\mathbf{H}$ . The signal-to-noise ratio (SNR) is defined as  $\gamma = E_m/N_0$ , where  $E_m$  is the average energy per transmission. The estimated CSI is denoted by  $\hat{\mathbf{H}}$ , and it is used to decode the transmitted signal. Based on the joint maximum likelihood detection in [5], the decoded information is obtained by:

$$\left[ \hat{t}_{\text{act}}, \hat{l} \right] = \arg \min_{t,l} \left\| \hat{\mathbf{h}}_t \chi_l \right\|^2 - 2\Re\{\mathbf{y}^H \hat{\mathbf{h}}_t \chi_l\}, \quad (8)$$

where  $\Re\{\cdot\}$  is an operator to extract the real part of a complex number.

## III. TRANSMISSION CROSS CHANNEL ESTIMATION

### A. Conventional Methods

In the conventional channel estimation (CCE) methods for SM, the transmit antennas are sequentially activated for sending the pilots. At the receiver, the channel information pertaining to the currently active antenna is estimated by a specific estimator such as least square (LS), minimum mean square error (MMSE), and recursive least square (RLS) [25]. In this paper, we consider LS in both CCE and the proposed method to ensure a fair comparison. Fig. 1 shows the pilot structure for CCE. During each blue colored slot, a pilot symbol is sent through the corresponding transmit antenna. Those slots are referred to as pilot slots. The remaining time slots are used to convey information-carrying symbols. The pilot ratio, denoted by  $\eta$ , is defined as the ratio of the number of pilots to the number of total symbols. The estimation period  $P_{\text{CE}}$  is defined as the interval between two adjacent

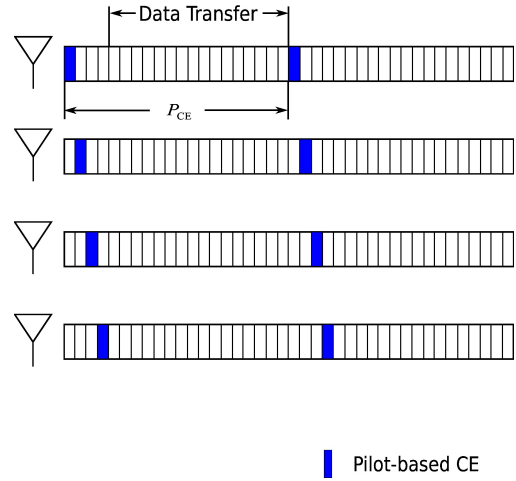


Fig. 1. Block diagram of CCE for SM with  $N_t = 4$

CE processes of any transmit antenna. The estimation period for CCE is given by:

$$P_{\text{CE}} = \frac{N_t T}{\eta}, \quad (9)$$

where  $T$  denotes the symbol period. It can be found that the CE period for CCE is proportional to the number of transmit antennas. We use  $q_t$  to denote the pilot symbol sent from the  $t$ -th transmit antenna, and the signal obtained at the  $r$ -th receive antenna is written as:

$$y_{r(n)} = h_{r,t(n)} q_t + w_r(n) \quad (10)$$

Since the channel estimation is individually implemented at each receive antenna, the index of receive antennas is omitted for the purpose of simplicity. The LS estimate for the  $t$ -th transmit antenna is then denoted by  $\tilde{h}_{t(n)}$ , and it is given by [25, p. 224, Eq. (8.9)]:

$$\tilde{h}_{t(n)} = \arg \min_h \|y_{(n)} - h q_t\|^2 \quad (11)$$

As both  $y_{(n)}$  and  $q_t$  are scalar, we have:

$$\tilde{h}_{t(n)} = \frac{y_{(n)}}{q_t} \quad (12)$$

After the channel information for all transmit antennas is obtained at the receiver, it is used to decode the data symbols until the next CE process comes. It is worth noting that, as the transmit antennas are activated sequentially, a gap exists between the pilot slot and the beginning of data transfer.

### B. Proposed Method

The channel difference information (CDI), denoted by  $\Delta J_{t_1, t_2} = h_{t_1} - h_{t_2}$ , is defined as the difference between the channel fading coefficients of two transmit antennas  $t_1$  and  $t_2$ . If CDI is known, then it is possible to obtain the full CSI of MIMO channels by estimating the channel information of any single transmit antenna. In the other words, only one transmit antenna is required to send the pilot signal to estimate the

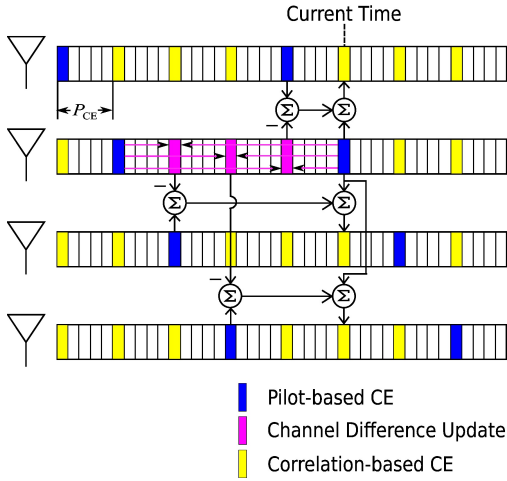


Fig. 2. Block diagram of TCCE for SM with  $N_t = 4$

entire MIMO channel. As a result, the CE time is significantly shortened in comparison with CCE.

A constant channel difference is however unrealistic. In order to make it available for time-varying channels, the channel difference information needs to keep updated. Taking four transmit antennas as an example, Fig. 2 depicts the block diagram of the proposed method. The pilot transmissions are represented by blue colored slots, similar as in Fig. 1. Note that, unlike CCE, the pilot slots pertaining to different transmit antennas are equally allocated along the time. At any pilot slot, the CSI of the currently active antenna is obtained in the same way as that of CCE. For those idle antennas, CSI is measured based on the estimated CSI of the active antenna and the CDI between the active antenna and the corresponding idle antenna. We refer to this type of CE as correlation-based CE, which is shown by yellow colored slots. The CDI for a certain idle antenna is calculated at the latest pilot slot of that antenna. The CSI of the currently active antenna at that slot, which is highlighted in pink color, is corrected by using interpolation based on the estimated CSIs at the current pilot slot and some previous pilot slots. At any pilot slot, the algorithm comprises four steps as follows:

1) *Pilot-based CE*: At first, the pilot-based CE is implemented for the currently active antenna, i.e.  $t_{act}$ . The corresponding estimation result is denoted by  $\tilde{h}_{t_{act}(n)}$ .

2) *Channel Difference Update*: For each transmit antenna, the pilot is conveyed once for every  $N_t$  pilot slots. At the previous  $N_t - 1$  pilot slots, the CSI of  $t_{act}$  is estimated by the correlation-based CE described in step 3. In this step, these CSIs are corrected by a low-pass interpolation based on  $\tilde{h}_{t_{act}(n)}$  and  $L-1$  previous estimates  $\tilde{h}_{t_{act}(n-lN_t/\eta)}$ ,  $l = 1, 2, \dots, L-1$ . The number of totally used estimates, i.e.  $L$ , is defined as the interpolation sequence length. The corrected CSI is denoted by  $\hat{h}_{t_{act}(n-k/\eta)}$ ,  $k = 1, 2, \dots, N_t - 1$ . For clarity, we choose the simplest case of  $L = 2$ , and it gives:

$$\hat{h}_{t_{act}(n-k/\eta)} = \left(1 - \frac{k}{N_t}\right) \tilde{h}_{t_{act}(n)} + \left(\frac{k}{N_t}\right) \tilde{h}_{t_{act}(n-N_t/\eta)}, \quad k = 1, 2, \dots, N_t - 1 \quad (13)$$

For  $L > 2$ , interested readers are referred to [26]. Regarding the  $t$ -th antenna, the last pilot-based CE happened at  $k_{t,t_{act}}/\eta$  slots before, where:

$$k_{t,t_{act}} = \begin{cases} t_{act} - t & \text{if } t \leq t_{act} \\ t_{act} - t + N_t & \text{if } t > t_{act} \end{cases} \quad (14)$$

The channel difference between  $t$  and  $t_{act}$  is updated as follows:

$$\Delta J_{t,t_{act}(n-k_{t,t_{act}}/\eta)} = \tilde{h}_{t(n-k_{t,t_{act}}/\eta)} - \tilde{h}_{t_{act}(n-k_{t,t_{act}}/\eta)} \quad (15)$$

3) *Correlation-based CE*: After collecting the CDI, it is possible to measure the CSI of the idle antennas. To be distinguished from pilot-based CE, the estimation result of correlation-based CE is denoted by  $\hat{h}_{t(n)}$  and it is obtained by:

$$\hat{h}_{t(n)} = \tilde{h}_{t_{act}(n)} + \Delta J_{t,t_{act}(n-k_{t,t_{act}}/\eta)}, \quad t \neq t_{act} \quad (16)$$

Substituting (13) and (15) into (16), we have:

$$\hat{h}_{t(n)} = \tilde{h}_{t(n-k_{t,t_{act}}/\eta)} + \frac{k_{t,t_{act}}}{N_t} \left( \tilde{h}_{t_{act}(n)} - \tilde{h}_{t_{act}(n-N_t/\eta)} \right), \quad t \neq t_{act} \quad (17)$$

Note that when  $t = t_{act}$  in (14), the value of  $k_{t,t_{act}}$  equals zero. Correspondingly, the right side of the above equation reduces to  $\tilde{h}_{t_{act}(n)}$ . Therefore, the estimated CSI obtained by both pilot-based CE and correlation-based CE can be written as the same expression in (17). We denote the estimated CSI of all transmit antennas as  $\hat{h}_{t(n)}$ , and rewrite (17) as:

$$\hat{h}_{t(n)} = \tilde{h}_{t(n-k_{t,t_{act}}/\eta)} + \frac{k_{t,t_{act}}}{N_t} \left( \tilde{h}_{t_{act}(n)} - \tilde{h}_{t_{act}(n-N_t/\eta)} \right), \quad t = 1, \dots, N_t \quad (18)$$

4) *Antenna Index Update*: The index of the transmit antenna to convey the pilot next time is then updated to:

$$t_{act} = \begin{cases} t_{act} + 1 & \text{if } t_{act} < N_t \\ 1 & \text{if } t_{act} = N_t \end{cases} \quad (19)$$

The flowchart of the proposed method is shown in Fig. 3, where the dash lines indicate the communications between the transmitter and the receiver. It is worth noting that there is no need for extra transmission or feedback in TCCE. Compared with CCE, the novel method only requires to store the previous estimation results at the receiver. The CE period for TCCE is computed by:

$$P_{CE} = \frac{T}{\eta}, \quad (20)$$

which is regardless of the number of transmit antennas used.

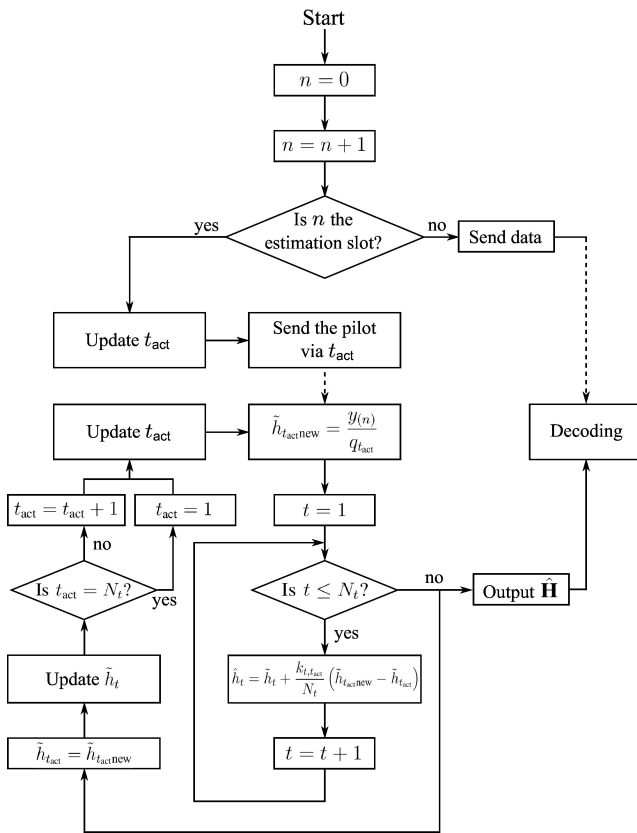


Fig. 3. Flowchart of the proposed CE method

#### IV. THEORETICAL ANALYSIS OF CHANNEL ESTIMATION ERRORS

In this section, we focus on analyzing the CE error, which is defined as the difference between the true CSI and its estimate. At the receiver, the CE errors can be thought of as an additive noise in addition to AWGN. The noise power, i.e. the CE error variance, affects the SNR together with AWGN. In this section: i) a framework is proposed to evaluate the CE errors for time-varying channels; ii) for both CCE and TCCE, a closed-form expression is derived for the distribution of the CE error.

##### A. Channel Estimation Error Modelling for Time-varying Channels

For a certain CE period, the CE error is denoted by  $\epsilon_{t(n)} = \hat{h}_t - h_{t(n)}$ , where  $\hat{h}_t$  is the constant channel estimation for that period, and  $h_{t(n)}$  is the actual CSI. For time-varying channels, a CE error consists of two parts: i) the error that occurs at the estimation point, which we refer to as the estimator error; ii) the error caused by the channel variation and this is referred to as the variation error. As the CE process is periodic, we focus on a single period and set the beginning of the estimation process to be the time origin. Then the estimator error is expressed by  $\epsilon_{t(0)} = \hat{h}_t - h_{t(0)}$ . It is presented in [27] that  $\epsilon_{t(0)}$  is a random variable (r.v.) with a distribution of  $\mathcal{CN}(0, \sigma_t^2)$ , where  $\sigma_t^2$  is the variance. We use  $\epsilon_{h(n)} = h_{t(0)} - h_{t(n)}$  to denote the variation error, and the CE error is therefore formulated as follows:

$$\epsilon_{t(n)} = \epsilon_{t(0)} + \epsilon_{h(n)} \quad (21)$$

The variation error can be rewritten as:

$$\epsilon_{h(n)} = \sum_{i=1}^n (h_{t(i-1)} - h_{t(i)}) \quad (22)$$

According to (4), we have:

$$h_{t(i)} = \sqrt{\alpha} h_{t(i-1)} + \sqrt{1-\alpha} h'_{t(i)} \quad (23)$$

Assuming the user speed in (5) does not exceed 50 m/s, this results in an  $\alpha \geq 0.989$ . Therefore, we can approximate  $\sqrt{\alpha} \approx 1$ . Substituting (23) into (22), it gives:

$$\epsilon_{h(n)} = -\sqrt{1-\alpha} \sum_{i=1}^n h'_{t(i)} \quad (24)$$

The variance of  $\epsilon_{h(n)}$  is denoted by  $\sigma_{h(n)}^2$ , and it is calculated by:

$$\sigma_{h(n)}^2 = n(1-\alpha) \quad (25)$$

Note that both  $\epsilon_{h(n)}$  and  $\epsilon_{t(0)}$  comply with the complex Gaussian distribution and they are independent of each other. Therefore, the CE error  $\epsilon_{t(n)}$  in (21) is distributed according to  $\mathcal{CN}(0, \sigma_t^2 + \sigma_{h(n)}^2)$ . The parameter  $\sigma_t^2$  for both CCE and the proposed method is studied in the following sections.

##### B. Conventional Channel Estimation

Based on (10) and (12), we obtain the estimator error of an LS estimator is  $\epsilon_{LS} = \frac{w}{q_t}$ . The variance of  $\epsilon_{LS}$  is the reciprocal of the SNR value, and we denote it by  $\sigma_{LS}^2 = \frac{1}{\gamma}$ . It is worth noting that for the  $t$ -th transmit antenna, the gap between the pilot slot and the beginning of data transfer is  $N_t - t$  slots. As a result, the parameter  $\sigma_t^2$  for CCE is calculated by:

$$\sigma_t^2 = \frac{1}{\gamma} + (N_t - t)(1-\alpha) \quad (26)$$

After completing the CE process, information-carried symbols are conveyed for the next  $N_t(N_d - 1)$  slots where  $N_d$  is the reciprocal of the pilot ratio. Combining (25) and (26), the variance of the CE error for CCE is obtained as follows:

$$\sigma_{\epsilon_{t(n)}}^2 = \frac{1}{\gamma} + (N_t - t + n)(1-\alpha), \quad n = 1, 2, \dots, N_t(N_d - 1) \quad (27)$$

##### C. Transmission Cross Channel Estimation

We denote the latest pilot slot in TCCE by  $n'$ . Since there is no gap between the pilot slot and the beginning of data transfer in TCCE, we have:

$$\epsilon_{t(0)} = \hat{h}_{t(n')} - h_{t(n')} \quad (28)$$

Substituting (18) and (24) into (28) results in (29).

$$\epsilon_{t(0)} = \underbrace{\sqrt{1-\alpha} \left( \frac{k_{t,t_{\text{act}}}}{N_t} \sum_{i=n'-N_t/\eta+1}^{n'-k_{t,t_{\text{act}}}/\eta} h'_{t_{\text{act}}(i)} \right)}_A + \underbrace{\sqrt{1-\alpha} \sum_{j=n'-k_{t,t_{\text{act}}}/\eta+1}^{n'} \left( \frac{k_{t,t_{\text{act}}}}{N_t} h'_{t_{\text{act}}(j)} - h'_{t(j)} \right)}_B + \underbrace{\frac{w(n'-k_{t,t_{\text{act}}})}{q_t} + \frac{k_{t,t_{\text{act}}}}{N_t} \left( \frac{w(n')}{q_{t_{\text{act}}}} + \frac{w(n'-N_t/\eta)}{q_{t_{\text{act}}}} \right)}_C \quad (29)$$

$$\sigma_{\epsilon_t(n)}^2 = \left\{ \left( \frac{k_{t,t_{\text{act}}}}{N_t} (1 - 2\rho_{t,t_{\text{act}}}) + 1 \right) \frac{k_{t,t_{\text{act}}}}{\eta} + n \right\} (1 - \alpha) + \left( 1 + 2 \left( \frac{k_{t,t_{\text{act}}}}{N_t} \right)^2 \right) \frac{1}{\gamma}, \quad n = 0, 1, \dots, N_d - 1 \quad (34)$$

$$\text{APEP}(\mathbf{x}_{t_{\text{act}},l} \rightarrow \mathbf{x}_{t,l'}) = \frac{1}{2\pi} \frac{\exp \left( -\frac{\gamma_l}{4} \text{vec} \left( \bar{\mathbf{H}}^H \right)^H \Lambda \left( \mathbf{I} + \frac{\gamma_l}{4} \mathbf{L}\Lambda \right)^{-1} \left( \bar{\mathbf{H}}^H \right)^H \right)}{|\mathbf{I} + \frac{\gamma_l}{4} \mathbf{L}\Lambda|} \quad (35)$$

**Proposition IV.1.** *Terms A, B, and C are independent of each other.*

*Proof:* Term C consists of all noise components, and hence it is straightforward to infer that term C is independent of the other two terms. The terms A and B contain partial information of  $\mathbf{H}'_{(i)}$  for different periods, i.e. different  $i$ . As stated,  $\mathbf{H}'_{(i)}$  and  $\mathbf{H}'_{(j)}$  are independent  $\forall i \neq j$ . Therefore, terms A and B are also independent. ■

Consequently, the variance of  $\epsilon_{t(0)}$  is the sum of the variances of terms A, B, and C. Similar to (25), the variance of A is obtained as follows:

$$\text{Var}(A) = \frac{N_t - k_{t,t_{\text{act}}}}{\eta} \left( \frac{k_{t,t_{\text{act}}}}{N_t} \right)^2 (1 - \alpha), \quad (30)$$

where  $\text{Var}(\cdot)$  is the variance of the variate in the brackets. Regarding term B, we denote  $\delta_{(i)} = k_{t,t_{\text{act}}} h'_{t_{\text{act}}(i)}/N_t - h'_{t(i)}$ .

**Proposition IV.2.** *The variance of  $\delta_{(i)}$  is  $\left( \frac{k_{t,t_{\text{act}}}}{N_t} \right)^2 + 1 - \frac{2\rho_{t_{\text{act}},t} k_{t,t_{\text{act}}}}{N_t}$ .*

*Proof:* See Appendix A. ■

The variance of term B is then calculated by:

$$\text{Var}(B) = \frac{k_{t,t_{\text{act}}}}{\eta} \left( \left( \frac{k_{t,t_{\text{act}}}}{N_t} \right)^2 + 1 - \frac{2\rho_{t_{\text{act}},t} k_{t,t_{\text{act}}}}{N_t} \right) (1 - \alpha) \quad (31)$$

Term C is the sum of noise components, and its variance is given by:

$$\text{Var}(C) = \left( 1 + 2 \left( \frac{k_{t,t_{\text{act}}}}{N_t} \right)^2 \right) \frac{1}{\gamma} \quad (32)$$

Adding (30), (31) and (32), the estimator error of TCCE for the  $t$ -th transmit antenna is formulated as follows:

$$\sigma_t^2 = \left( \frac{k_{t,t_{\text{act}}}}{N_t} (1 - 2\rho_{t,t_{\text{act}}}) + 1 \right) \frac{k_{t,t_{\text{act}}}}{\eta} (1 - \alpha) + \left( 1 + 2 \left( \frac{k_{t,t_{\text{act}}}}{N_t} \right)^2 \right) \frac{1}{\gamma} \quad (33)$$

Note that TCCE-based SM conveys  $(N_d - 1)$  symbols after each estimation. The variance of the CE error for TCCE is calculated by (34).

## V. ABEP BOUND FOR SM WITH PRACTICAL CHANNEL ESTIMATES

Some research has been conducted on the BER performance analysis for SM in the presence of CE errors, e.g. [12]. In the SOTA literature, however, the distribution of CE errors for all transmit antennas are assumed to be identical. In fact, in both CCE and TCCE, the distribution of CE errors is related to the index of transmit antennas. Based on an existing ABEP bound for SM with perfect CSI, we derive a closed-form ABEP bound in the case of practical channel estimations, where the CE errors for different transmit antennas are considered to have different variances.

### A. ABEP Bound for SM with Perfect CSI

With the assumption of perfect CSI, a closed-form ABEP bound for SM is proposed in [28]. When the signal  $\mathbf{x}_{t_{\text{act}},l}$  is transmitted, the conditional average pair-wise probability (APEP) of deciding on  $\mathbf{x}_{t,l'}$  is given by [28, Eq. (22)] as in (35). The parameter  $\gamma_l$  denotes the SNR for the symbol  $\chi_l$ , and:

$$\Lambda = \mathbf{R}_r \otimes (\Psi \Psi^H \mathbf{R}_t), \quad (36)$$

where  $\Psi = (\mathbf{x}_{t_{\text{act}},l} - \mathbf{x}_{t,l'})$ , and  $\otimes$  is the Kronecker product. The parameters  $\bar{\mathbf{H}}$  and  $\mathbf{L}$  are the mean and the covariance matrix of  $\mathbf{H}$ , respectively. In the case of Rayleigh fading, we



have  $\bar{\mathbf{H}} = \mathbf{0}_{N_r \times N_t}$  which is an  $N_r \times N_t$  all zeros matrix, and  $\mathbf{L} = \mathbf{I}_{N_r N_t}$  where  $\mathbf{I}_n$  is an  $n \times n$  identity matrix. The vectorization operator  $\text{vec}(\cdot)$  stacks the columns of the matrix in a column vector.

Consequently, the ABEP for SM can be approximated by using the union bound [29], and this gives:

$$\text{ABEP} \leq \frac{1}{2^{\eta_s}} \sum_{t_{\text{act}}, l} \sum_{t', l'} \frac{N(\mathbf{x}_{t_{\text{act}}, l} \rightarrow \mathbf{x}_{t', l'})}{\eta_s} \text{APEP}(\mathbf{x}_{t_{\text{act}}, l} \rightarrow \mathbf{x}_{t', l'}), \quad (37)$$

where  $N(\mathbf{x}_{t_{\text{act}}, l} \rightarrow \mathbf{x}_{t', l'})$  is the number of bits in error between  $\mathbf{x}_{t_{\text{act}}, l}$  and  $\mathbf{x}_{t', l'}$ .

### B. ABEP Bound for SM with Practical Channel Estimates

There are two aspects of the effect of CE errors on decoding: i) the CE error of the currently active antenna, and ii) the CE error of the idle antenna that is incorrectly decoded. The effective SNR  $\gamma_{\text{eff}}$  is defined as the SNR that considers both the CE error and AWGN as the noise, and it is formulated as follows:

$$\gamma_{\text{eff}}(\mathbf{x}_{t_{\text{act}}, l} \rightarrow \mathbf{x}_{t', l'}) = \frac{\gamma_l}{1 + \sigma_{\epsilon_t}^2 + \gamma_l \sigma_{\epsilon_{t_{\text{act}}}}^2}, \quad (38)$$

where  $\sigma_{\epsilon_t}^2$  is the average of the variances of the CE error for the  $t$ -th transmit antenna. It is worth noting that  $\sigma_{\epsilon_{t_{\text{act}}}}^2$  and  $\sigma_{\epsilon_t}^2$  affect the effective SNR in different ways. Since the signal is sent through  $t_{\text{act}}$ , the noise caused by its CE error is the product of the transmit power and  $\sigma_{\epsilon_{t_{\text{act}}}}^2$ . The ABEP bound for SM associated with a practical CE method can be obtained by replacing  $\gamma_l$  in (35) with  $\gamma_{\text{eff}}$ .

## VI. SIMULATION RESULTS

In this section, Monte Carlo simulation results are presented to validate the performance of the proposed CE approach. The framework for the CE errors and the proposed ABEP bound are verified. Further, the BER performance of SM using TCCE is compared with CCE. Different numbers of transmit antennas are considered. To ensure a fair comparison, the antennas are located in a matrix with a normalized diagonal distance. The correlation coefficient between the two ends of the diagonal is thought of as the reference correlation [30], which is denoted by  $\rho_{\text{tx}}$ . Based on this, the effect of channel correlations on both CCE and TCCE is also studied. Furthermore, we analyze the BER performance of SM under different user speeds. A pilot ratio of 5% is assumed in all simulations [31]. The user speed is fixed to be 5 m/s, except when studying its effect.

### A. The Distribution of Channel Estimation Errors

At first, we study the CE error in terms of probability density function (PDF). The main purpose is to validate the analytical framework proposed in Section IV. The derivation in (34) shows that the CE performance of the proposed method only depends on  $N_t$ , SNR and channel correlation, regardless of  $N_r$  and  $\eta_s$ . Taking  $N_t = 8$ ,  $\gamma = 20$  dB and  $\rho_{\text{tx}} = 0.5$  as an example, the PDFs of the CE errors for CCE and TCCE are shown in Fig. 4 and Fig. 5, respectively. As mentioned

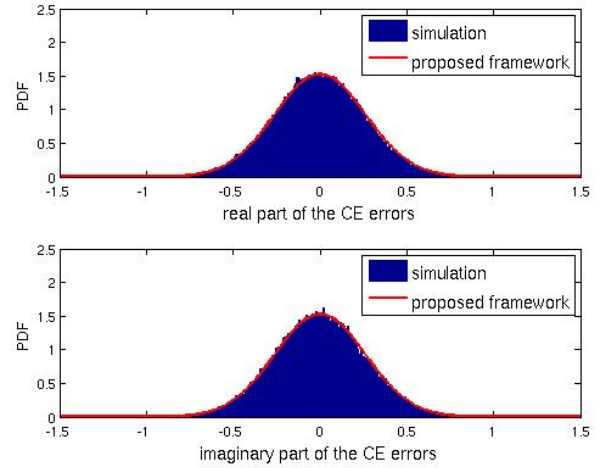


Fig. 4. PDF of the CE errors for CCE

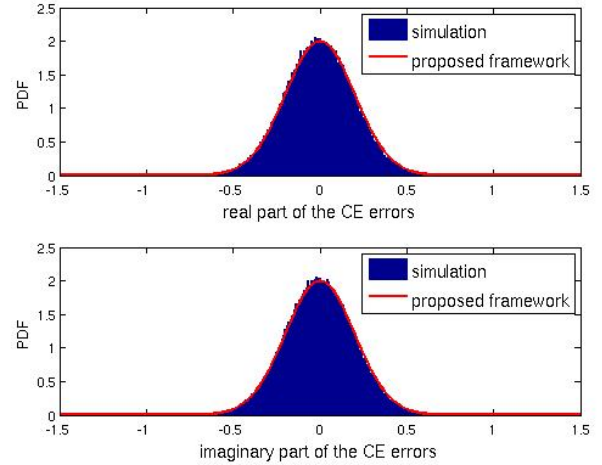


Fig. 5. PDF of the CE errors for TCCE

previously, the CE error is a complex variate like AWGN. Therefore, in each figure, the results for the real part and the imaginary part of errors are depicted separately. As shown, the CE errors present a zero-mean complex Gaussian distribution, and the theoretical PDF matches the simulation results very well. Another finding is that the CE errors of TCCE are closer to their expectation than that of CCE. In other words, the variance of CE errors in TCCE is smaller than that in CCE. This signifies that, in this case, TCCE offers a more accurate CE for SM than CCE.

### B. ABEP Bound for SM based on TCCE

Secondly, we focus on validating the proposed ABEP bound for SM with practical channel estimates in Section V. Assuming  $N_t = 4$ , Fig. 6 and Fig. 7 show the BER performance of SM based on TCCE for uncorrelated channels and correlated channels, respectively. Two values of  $\eta_s$ , 3 bits per channel per user (bpcu) and 4 bpcu, are considered. It can be observed that in both cases, the analytical bound is tightly close to the simulations. Additionally, the BER performance tends towards



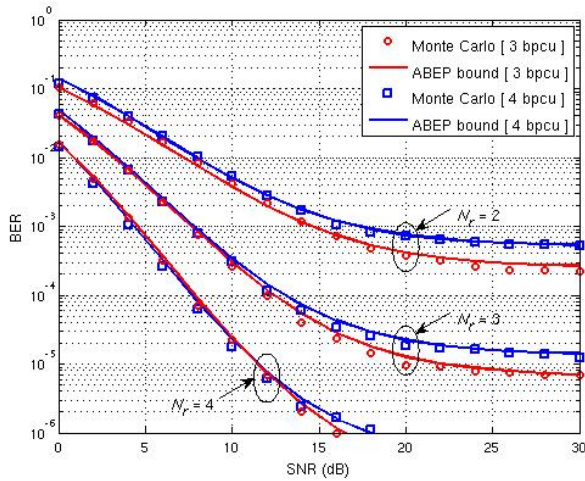


Fig. 6. BER of SM using TCCE over uncorrelated Rayleigh fading channels. (Line) Analytical bound, (Dot) Simulation.

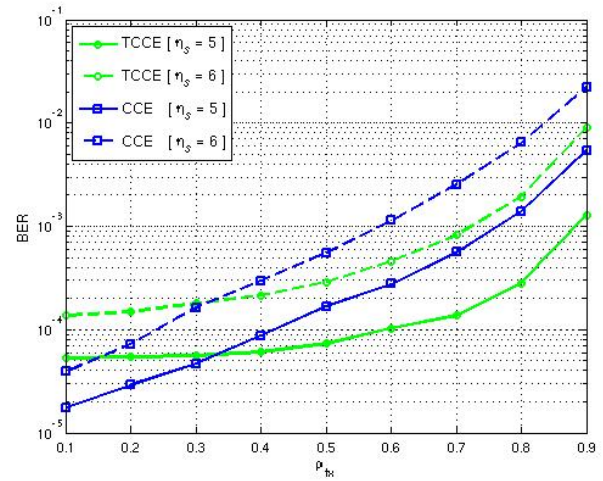


Fig. 8. BER performance of SM in terms of  $\rho_{tx}$ . The SNR is assumed to be 20 dB.

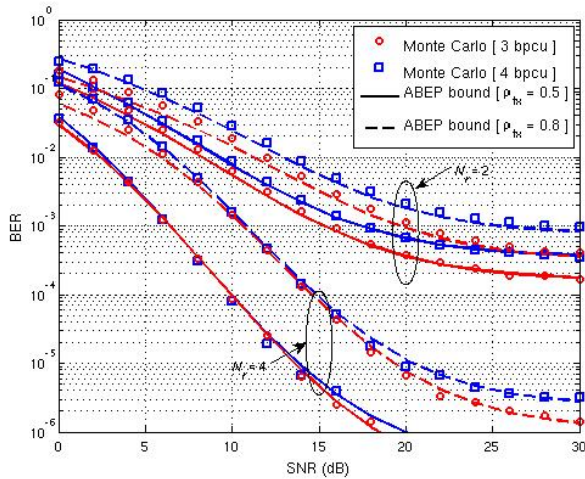


Fig. 7. BER of SM using TCCE over correlated Rayleigh fading channels. (Line) Analytical bound, (Dot) Simulation.

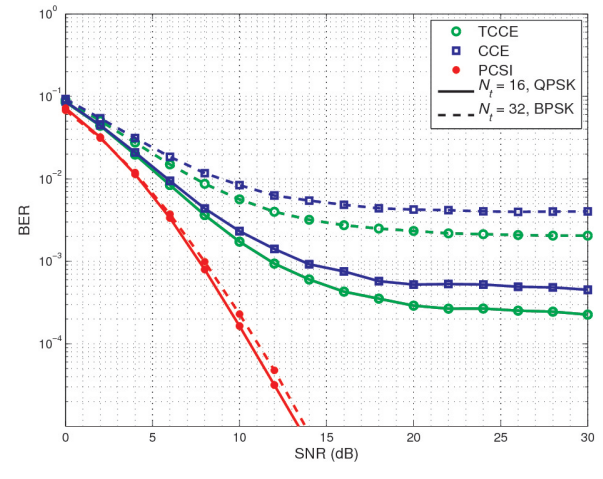


Fig. 9. BER performance of SM in terms of SNR. A medium channel correlation of  $\rho_{tx} = 0.5$  is considered.

stability with an increase of SNR. When SNR is larger than 25 dB, the BER curve becomes almost flat and a limit is put on the achievable BER. The reason for this trend is that the CE error becomes the dominant factor instead of noise.

### C. BER Comparison with CCE

Thirdly, the BER performance of TCCE is compared with CCE in three aspects: the channel correlation, the number of transmit antennas, and the user speed. In order to focus on studying the effect of the above factors, the number of receive antennas is assumed to be four in all comparisons.

1) *Effect of Channel Correlation:* Fig. 8 shows the BER performance of TCCE and CCE as a function of the channel correlation. Sixteen transmit antennas and an SNR of 20 dB are assumed. As shown in Fig. 8, the proposed approach falls behind CCE when the correlation coefficient  $\rho_{tx}$  is smaller than 0.3. The reason is that the performance of TCCE relies on the channel correlation. For a low channel correlation, it is

difficult to track the channel difference information between transmit antennas. However, when the parameter  $\rho_{tx}$  is larger than 0.4, TCCE offers a much better BER performance than CCE. Similar, but less pronounced trends are noticed at lower SNRs. Based on the above analysis, an adaptive CE technique is available for SM by switching between CCE and TCCE.

2) *Effect of the Number of Transmit Antennas:* Assuming different numbers of transmit antennas, the BER performance of SM for  $\rho_{tx} = 0.5$  and  $\rho_{tx} = 0.8$  is shown in Fig. 9 and Fig. 10, respectively. The parameter  $\eta_s$  is fixed to be six to ensure a fair comparison. Additionally, the case of perfect CSI (PCSI) is considered as a benchmark.

The following outcomes are observed: i) compared with CCE, the BER performance of TCCE is much closer to that of PCSI; ii) when  $N_t$  increases, the BER performance for both CE methods degrades more rapidly than PCSI. However, the reasons for CCE and TCCE are different. The CE period of CCE is proportional to  $N_t$ , and therefore, the CE results become less accurate when more transmit antennas are used.

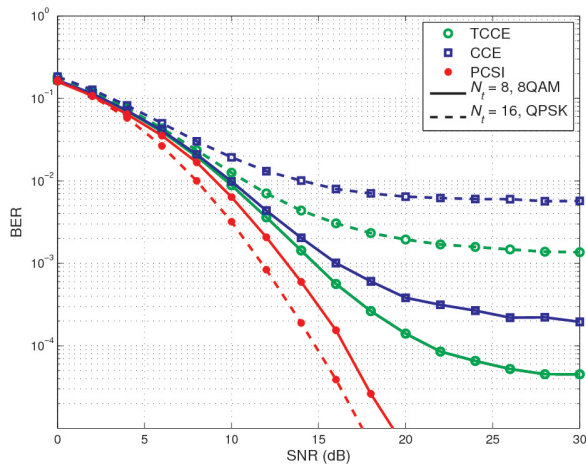


Fig. 10. BER performance of SM in terms of SNR. A high channel correlation of  $\rho_{tx} = 0.8$  is considered.

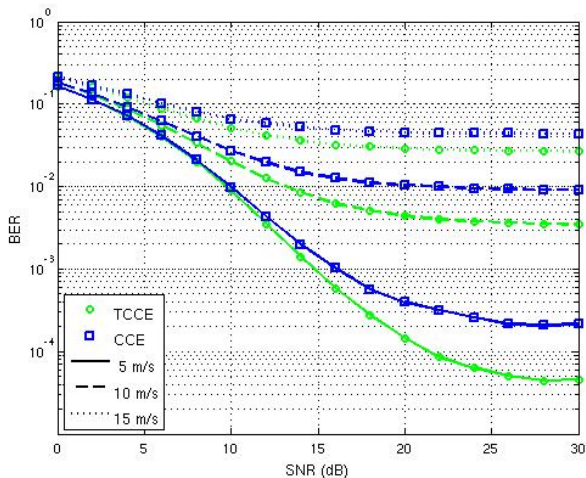


Fig. 11. BER performance of SM in terms of SNR for various user speeds. The parameter  $\rho_{tx}$  is assumed to be 0.8

Unlike in CCE, the CE period of TCCE is irrelevant to  $N_t$ . However, with an increase of  $N_t$ , the interval between two adjacent pilot slots for a certain transmit antenna is increased. This results in a less accurate channel difference information, which causes a performance degradation in the correlation-based CE. Furthermore, in a comparison to CCE, the energy gain achieved by TCCE becomes greater as  $N_t$  increases. Given  $\rho_{tx} = 0.8$  and  $N_t = 8$ , for example, an SNR gain of 2.8 dB is obtained by TCCE to achieve the same BER value of CCE at  $\gamma = 20$  dB. While  $N_t = 16$ , this gain is increased to 7.5 dB.

3) *Effect of User Speed:* The user speed directly affects the coherence time in time-varying channels, and therefore, it is essential to study its effect on the CE performance. Assuming  $\rho_{tx} = 0.8$  and  $N_t = 8$ , Fig. 11 shows the BER performance of SM for different user speeds. The following outcomes are observed: i) for both CCE and TCCE, the BER performance degrades as the user speed increases; ii) with an increase of the

user speed, the difference between the performance of TCCE and CCE diminishes. The reason for this trend is that when the channel varies very rapidly, all CE techniques would fail to perform properly for a fixed pilot ratio. Nevertheless, TCCE still outperforms CCE in a significant way for a high user speed. In the case of 15 m/s, for example, CCE reaches its achievable BER of 5% at  $\gamma = 15$  dB. Meanwhile, TCCE requires only 10 dB to achieve the same BER value, which provides an SNR gain of 5 dB when compared with CCE.

## VII. CONCLUSIONS

In this paper, we propose a novel CE method that aims to improve the performance for SM over correlated fading channels. The basic concept of this new approach is to track the channel difference information between transmit antennas, and estimate the entire channel by sending the pilot signal through only one antenna. Therefore, the CE period of the proposed method depends on the pilot ratio only, regardless of the number of transmit antennas used. Further, we propose an analytical framework for the distribution of CE errors in time-varying channels, and the corresponding ABEP bound for SM based on the a practical CE method. Simulation results show that for medium and high channel correlations, TCCE achieves an SNR gain of up to 7.5 dB in comparison with CCE. When the channel correlation is very low, TCCE performs worse than CCE because the channel difference information is difficult to track in this situation. By switching between CCE and TCCE, an adaptive CE technique is available for SM that is a promising MIMO scheme for future communication systems.

## APPENDIX A

For two complex variates  $X$  and  $Y$ , the variance of their sum is given by:

$$\text{Var}(X + Y) = \text{Var}(X) + \text{Var}(Y) + 2\text{Cov}(XY), \quad (39)$$

where  $\text{Cov}(X, Y) = \mathbf{E}[(X - \mu_X)(Y - \mu_Y)^*]$  is the covariance of  $X$  and  $Y$ ;  $\mathbf{E}[\cdot]$  is the mathematical expectation;  $\mu_X$  and  $\mu_Y$  are the means of  $X$  and  $Y$ , respectively;  $(\cdot)^*$  is the conjugate operator. Therefore, the variance of  $\delta_{(i)}$  is formulated as follows:

$$\begin{aligned} \text{Var}(\delta_{(i)}) &= \left(\frac{k_{t,t_{\text{act}}}}{N_t}\right)^2 \text{Var}(h'_{t_{\text{act}}(i)}) + \text{Var}(-h'_{t(i)}) \\ &\quad + 2\text{Cov}\left(\frac{k_{t,t_{\text{act}}}}{N_t} h'_{t_{\text{act}}(i)}, (-h'_{t(i)})\right) \end{aligned} \quad (40)$$

Since  $h'_{t_{\text{act}}(i)}$  and  $h'_{t(i)}$  are both zero-mean complex Gaussian random variables with variance of one, so we have  $\text{Var}(h'_{t_{\text{act}}(i)}) = 1$  and  $\text{Var}(-h'_{t(i)}) = 1$ . Using the definition of covariance, the covariance part in (40) is computed by:

$$\text{Cov}\left(\frac{k_{t,t_{\text{act}}}}{N_t} h'_{t_{\text{act}}(i)}, (-h'_{t(i)})\right) = -\frac{k_{t,t_{\text{act}}}}{N_t} \mathbf{E}\left[h'_{t_{\text{act}}(i)} (h'_{t(i)})^*\right] \quad (41)$$



Note that, because the means of  $h'_{t_{\text{act}}(i)}$  and  $h'_{t(i)}$  are zeros,  $\mathbf{E} \left[ h'_{t_{\text{act}}(i)} \left( h'_{t(i)} \right)^* \right]$  is exactly the covariance of  $h'_{t_{\text{act}}(i)}$  and  $h'_{t(i)}$ . According to the definition of correlation, we have:

$$\rho_{t,t_{\text{act}}} = \frac{\text{Cov}(h'_{t_{\text{act}}(i)}, h'_{t(i)})}{\sqrt{\text{Var}(h'_{t_{\text{act}}(i)})\text{Var}(h'_{t(i)})}} \quad (42)$$

Therefore, the covariance part in (40) is obtained by:

$$\text{Cov} \left( \frac{k_{t,t_{\text{act}}}}{N_t} h'_{t_{\text{act}}(i)}, \left( -h'_{t(i)} \right) \right) = -\frac{k_{t,t_{\text{act}}}}{N_t} \rho_{t,t_{\text{act}}} \quad (43)$$

The variance of  $\delta_{(i)}$  is then computed by:

$$\text{Var}(\delta_{(i)}) = \left( \frac{k_{t,t_{\text{act}}}}{N_t} \right)^2 + 1 - \frac{2\rho_{t,t_{\text{act}}} k_{t,t_{\text{act}}}}{N_t} \quad (44)$$

#### ACKNOWLEDGEMENT

We gratefully acknowledge support from the European Union's Seventh Framework Programme (FP7) under grant agreement No. 264759 (GREENET Project).

#### REFERENCES

- [1] X. Wu, M. Di Renzo, and H. Haas, "Channel estimation for spatial modulation," in *24th IEEE International Symposium on Personal Indoor and Mobile Radio Commun. (PIMRC)*, Sept. 2013, pp. 306–310.
- [2] R. Mesleh, H. Haas, S. Sinanovic, C. W. Ahn, and S. Yun, "Spatial modulation," *IEEE Trans. Veh. Technol.*, vol. 57, no. 4, pp. 2228–2241, July 2008.
- [3] R. Mesleh, H. Haas, C. W. Ahn, and S. Yun, "Spatial modulation - a new low complexity spectral efficiency enhancing technique," in *1st International Conference on Commun. and Networking in China (ChinaCom)*, Oct. 2006, pp. 1–5.
- [4] M. Di Renzo, H. Haas, and P. M. Grant, "Spatial modulation for multiple-antenna wireless systems: A survey," *IEEE Commun. Mag.*, vol. 49, no. 12, pp. 182–191, Dec. 2011.
- [5] J. Jeganathan, A. Ghrayeb, and L. Szczecinski, "Spatial modulation: Optimal detection and performance analysis," *IEEE Commun. Lett.*, vol. 12, no. 8, pp. 545–547, Aug. 2008.
- [6] M. Di Renzo and H. Haas, "Performance analysis of spatial modulation," in *5th International Conference on Communications and Networking in China (CHINACOM)*, Aug. 2010, pp. 1–7.
- [7] M. Di Renzo and H. Haas, "Bit error probability of SM-MIMO over generalized fading channels," *IEEE Trans. Veh. Technol.*, vol. 61, no. 3, pp. 1124–1144, March 2012.
- [8] M. Biguesh and A. B. Gershman, "Training-based MIMO channel estimation: A study of estimator tradeoffs and optimal training signals," *IEEE Trans. Signal Proc.*, vol. 54, no. 3, pp. 884–893, March 2006.
- [9] P. Wolniansky, G. Foschini, G. Golden, and R. Valenzuela, "V-BLAST: An architecture for realizing very high data rates over the rich-scattering wireless channel," in *1998 International Symposium on Signals, Systems, and Electronics (ISSSE)*, Sept. 1998, pp. 295–300.
- [10] V. Tarokh, H. Jafarkhani, and A. Calderbank, "Space-time block codes from orthogonal designs," *IEEE Trans. Inf. Theory*, vol. 45, no. 5, pp. 1456–1467, July 1999.
- [11] M. Koca and H. Sari, "Performance of spatial modulation over correlated fading channels with channel estimation errors," in *2013 IEEE Wireless Communications and Networking Conference (WCNC)*, April 2013, pp. 3937–3942.
- [12] E. Basar, U. Aygolu, E. Panayirci, and H. Poor, "Performance of spatial modulation in the presence of channel estimation errors," *IEEE Commun. Lett.*, vol. 16, no. 2, pp. 176–179, Feb. 2012.
- [13] M. Di Renzo, D. De Leonardi, F. Graziosi, and H. Haas, "Space shift keying (SSK-) MIMO with practical channel estimates," *IEEE Trans. Commun.*, vol. 60, no. 4, pp. 998–1012, April 2012.
- [14] M. Faiz, S. Al-Ghadhban, and A. Zerguine, "Recursive least-squares adaptive channel estimation for spatial modulation systems," in *9th IEEE Malaysia International Conference on Commun. (MICC)*, Dec. 2009, pp. 785–788.

- [15] S. Sugiura and L. Hanzo, "Effects of channel estimation on spatial modulation," *IEEE Signal Processing Lett.*, vol. 19, no. 12, pp. 805–808, Dec. 2012.
- [16] J. H. Kotecha and A. Sayeed, "Transmit signal design for optimal estimation of correlated MIMO channels," *IEEE Trans. Signal Processing*, vol. 52, no. 2, pp. 546–557, Feb. 2004.
- [17] N. Shariati, J. Wang, and M. Bengtsson, "Robust training sequence design for correlated MIMO channel estimation," *IEEE Trans. Signal Processing*, vol. 62, no. 1, pp. 107–120, Jan. 2014.
- [18] C.-T. Chiang and C. Fung, "Robust training sequence design for spatially correlated MIMO channel estimation," *IEEE Trans. Veh. Technol.*, vol. 60, no. 7, pp. 2882–2894, Sept. 2011.
- [19] Y. H. Kho and D. Taylor, "MIMO channel estimation and tracking Based on polynomial prediction with application to equalization," *IEEE Trans. Veh. Technol.*, vol. 57, no. 3, pp. 1585–1595, May 2008.
- [20] Y.-C. Chen and Y.-T. Su, "MIMO channel estimation in correlated fading environments," *IEEE Trans. Wireless Commun.*, vol. 9, no. 3, pp. 1108–1119, March 2010.
- [21] D. Angelosante, E. Biglieri, and M. Lops, "Sequential estimation of multipath MIMO-OFDM channels," *IEEE Trans. Signal Processing*, vol. 57, no. 8, pp. 3167–3181, Aug. 2009.
- [22] C. Oestges, "Validity of the Kronecker model for MIMO correlated channels," in *63rd IEEE Veh. Technol. Conf. (VTC Spring)*, vol. 6, May 2006, pp. 2818–2822.
- [23] S. Loyka, "Channel capacity of MIMO architecture using the exponential correlation matrix," *IEEE Commun. Lett.*, vol. 5, no. 9, pp. 369–371, Sept. 2001.
- [24] C. Peel and A. Swindlehurst, "Performance of space-time modulation for a generalized time-varying Rician channel model," *IEEE Trans. Wireless Commun.*, vol. 3, no. 3, pp. 1003–1012, May 2004.
- [25] S. M. Kay, *Fundamentals of Statistical Signal Processing: Estimation Theory*, 1st ed. Prentice Hall PTR, 1993.
- [26] M. Hazewinkel, *Linear Interpolation*, 1st ed. Springer, 2001.
- [27] J. Wu and C. Xiao, "Optimal diversity combining based on linear estimation of Rician fading channels," *IEEE Trans. Commun.*, vol. 56, no. 10, pp. 1612–1615, Oct. 2008.
- [28] A. Younis, D. A. Basnayaka, and H. Haas, "Performance analysis for generalised spatial modulation," in *20th European Wireless Conference*, May 2014.
- [29] P. J.G., *Digital Communications*, 4th ed. McGraw-Hill, 2000.
- [30] H. Kim, H. Kim, N. Kim, H. Park, S. Seo, and J. Choi, "Efficient transmit antenna selection for correlated MIMO channels," in *2009 IEEE Wireless Communications and Networking Conference (WCNC)*, April 2009, pp. 1–5.
- [31] J. Berkmann, C. Carbonelli, F. Dietrich, C. Drewes, and W. Xu, "On 3G LTE terminal implementation - standard, algorithms, complexities and challenges," in *2008 International Wireless Communications and Mobile Computing Conference (IWCMC)*, Aug. 2008, pp. 970–975.



**Xiping Wu** received the B.Sc. degree from Southeast University, Nanjing, China in 2008 and the M.Sc. degree with distinction from the University of Edinburgh, Scotland, United Kingdom in 2011. From September 2011 to August 2014, he was Marie-Curie Early-Stage Researcher (ESR) as well as Ph.D. candidate at the University of Edinburgh, funded by the European Union's Seventh Framework Programme (FP7) project GREENET. From December 2013 to April 2014, he was on secondment to the Department of Electrical and Information Engineering, University of L'Aquila, Italy. Since September 2014, he has been Research Associate with the Institute for Digital Communications (IDCOM), the University of Edinburgh, funded by British Engineering and Physical Sciences Research Council (EPSRC). His main research interests are in the areas of wireless communication theory, visible light communications, and wireless network management. In 2010, he was granted the Scotland Saltire Scholarship by the Scottish Government.



**Holger Claussen** received his Ph.D. degree in signal processing for digital communications from the University of Edinburgh, United Kingdom in 2004. He is author of more than 70 publications and 100 filed patent applications. He is senior member of the IEEE, and member of the IET.

Dr. Holger Claussen is leader of Small Cells Research at Bell Labs, Alcatel-Lucent. In this role, he and his team are innovating in all areas related to future evolution, deployment, and operation of small cell networks to address the exponential growth in mobile data traffic. His research in this domain has been commercialized in Alcatel-Lucent's Small Cell product portfolio and continues to have significant impact. Prior to this, Holger was head of the Autonomous Networks and Systems Research Department at Bell Labs Ireland, where he directed research in the area of self-managing networks to enable the first large scale femtocell deployments from 2009 onwards. During this time, he also built a cloud computing research team, focusing on predictable performance and reducing latency to enable running telecommunication applications on a cloud infrastructure. Holger joined Bell Labs in 2004 and began his research in the areas of auto-configuration and dynamic optimization of networks, flat cellular network architectures, user mobility, resource management, end-to-end network modeling and improving the energy efficiency of networks.



**Harald Haas** received the PhD degree from the University of Edinburgh in 2001. He currently holds the Chair of Mobile Communications at the University of Edinburgh. His main research interests are in optical wireless communications, hybrid optical wireless and RF communications, spatial modulation, and interference coordination in wireless networks. He first introduced and coined "spatial modulation" and "Li-Fi". Li-Fi was listed among the 50 best inventions in TIME Magazine 2011.

Prof Haas was an invited speaker at TED Global 2011, and his talk has been watched online more than 1.5 million times. He is co-founder and chief scientific officer (CSO) of pureLiFi Ltd. Professor Haas holds 31 patents and has more than 30 pending patent applications. He has published 300 conference and journal papers including a paper in Science. He was co-recipient of a best paper award at the IEEE Vehicular Technology Conference in Las Vegas in 2013. In 2012, he was the only recipient of the prestigious Established Career Fellowship from the EPSRC (Engineering and Physical Sciences Research Council) within Information and Communications Technology in the UK. Haas is recipient of the Tam Dalyell Prize 2013 awarded by the University of Edinburgh for excellence in engaging the public with science. In 2014, he was selected by EPSRC as one of ten RISE (Recognising Inspirational Scientists and Engineers) Leaders.



**Marco Di Renzo** (S'05-AM'07-M'09-SM'14) received the Laurea (cum laude) and the Ph.D. degrees in Electrical and Information Engineering from the Department of Electrical and Information Engineering, University of L'Aquila, Italy, in April 2003 and in January 2007. In October 2013, he received the Habilitation à Diriger des Recherches (HDR) from the University of Paris-Sud XI, Paris, France. Since January 2010, he has been a Tenured Academic Researcher ("Chargé de Recherche Titulaire") with the French National Center for Scientific Research

(CNRS), as well as a faculty member of the Laboratory of Signals and Systems (L2S), a joint research laboratory of the CNRS, the École Supérieure d'Électricité (SUPÉLEC) and the University of Paris-Sud XI, Paris, France. His main research interests are in the area of wireless communications theory.

Dr. Di Renzo is a recipient of several awards, which include a special mention for the outstanding five-year (1997-2003) academic career, University of L'Aquila, Italy; the THALES Communications fellowship (2003-2006), University of L'Aquila, Italy; the 2004 Best Spin-Off Company Award, Abruzzo Region, Italy; the 2006 DEWS Travel Grant Award, University of L'Aquila, Italy; the 2008 Torres Quevedo Award, Ministry of Science and Innovation, Spain; the "Dérogação pour l'Encadrement de Thèse" (2010), University of Paris-Sud XI, France; the 2012 IEEE CAMAD Best Paper Award; the 2012 IEEE WIRELESS COMMUNICATIONS LETTERS Exemplary Reviewer Award; the 2013 IEEE VTC-Fall Best Student Paper Award; the 2013 Network of Excellence NEWCOM# Best Paper Award; the 2013 IEEE TRANSACTIONS ON VEHICULAR TECHNOLOGY Top Reviewer Award; the 2013 IEEE-COMSOC Best Young Researcher Award for Europe, Middle East and Africa (EMEA Region); and the 2014 IEEE ICNC Single Best Paper Award Nomination (Wireless Communications Symposium). Currently, he serves as an Editor of the IEEE COMMUNICATIONS LETTERS and of the IEEE TRANSACTIONS ON COMMUNICATIONS (Heterogeneous Networks Modeling and Analysis).